

Revisiting the epoch of cosmic acceleration

David Dahiya* and Deepak Jain**

*Technische Universität Dresden, 01069 Dresden, Germany

**Deen Dayal Upadhyaya College, University of Delhi, Dwarka, New Delhi, India

Received 20xx month day; accepted 20xx month day

Abstract We revisit the epoch of cosmic speed-up characterized by the redshift of transition from a decelerated to an accelerated phase. This redshift is termed the transition redshift (z_t). We use the spatially Flat and Non-Flat variants of the most common Λ CDM and XCDM models to put constraints on the transition redshift along with the other model parameters. The data for this analysis comes from the recent and updated Pantheon+ Supernova (SNe) dataset and the Hubble parameter measurements obtained from Cosmic Chronometers (CC). We consider both datasets with their respective covariance matrices incorporating all statistical and systematic uncertainties. We observe that using the combined datasets of $H(z)$ and SNe, the best fit value of transition redshift lies in the range $0.61 < z_t < 0.82$ for all four dark energy models. Incidentally, we observe a positive curvature for the Non-Flat models, correlations between several model parameters and a strong degeneracy between the curvature and the equation of state parameter.

Key words: Cosmological Parameters — cosmology: observations — Dark Energy

1 INTRODUCTION

The 1998 study of very distant supernovae provided irrefutable proof that, at present, the universe is undergoing an accelerated expansion. (Riess et al., 1998; Perlmutter et al., 1999). Through high-redshift supernovae, it was established that the early universe was dominated by non-relativistic matter, which supports a decelerating expansion of the universe. Thus, it was apparent that, at a certain epoch, the expansion of the universe shifted from a decelerating phase to an accelerated one. This epoch is characterized by the transition redshift and denoted by the parameter z_t . It is suggested that z_t may be a new fundamental cosmological parameter (along with H_0 and q_0) that aids in understanding the evolution of cosmic expansion (Lima et al., 2012; Melchiorri et al., 2007).

* E-Mail: davddahiya@gmail.com

In recent years, with the influx of new data, several model-independent and model-dependent approaches have been formulated to constrain the transition redshift and other parameters. The model-independent approach does not make any assumptions about the composition of the universe or the theory of gravitation other than assuming a metric structure. This approach involves parameterizations and reconstructions of different kinematic variables, including the Hubble parameter $H(z)$, the deceleration parameter $q(z)$, and the equation of state parameter $\omega(z)$ in a model independent way (Al Mamon, 2021; Çamlıbel et al., 2020; Seikel et al., 2012). For instance, Rani et al. (2015) used three different parameterizations of the deceleration parameter and a local regression method to extrapolate the Hubble parameter and obtained a $z_t \in [0.60, 0.98]$ (Rani et al., (2015)). Similarly, Jesus et al. (2018) measured a $z_t \in [0.806, 0.973]$ using different polynomial parameterizations of the comoving distance $D_C(z)$, $H(z)$ and $q(z)$ (J.F. Jesus et al., 2018). On the other hand, (Jesus et al., 2020) used Gaussian process to reconstruct $H(z)$ and the luminosity distance, $D_L(z)$. They obtained transition redshift as 0.59 and 0.683 for the two reconstructions respectively. For a similar reconstruction of $H(z)$, Toribio and Fabris (2020) obtained a $z_t \sim 0.7$ (Velasquez-Toribio & Fabris, 2021). Capozziello et al. (2022) measured a $z_t \in [0.473, 1.183]$ after performing a more recent reconstruction of $H(z)$ and $q(z)$ using SNe and Hubble data (Capozziello et al., 2021). More methods and parameterization for obtaining z_t can be found in (Kumar et al., 2022; Koussour et al., 2022; Muccino et al., 2022; Cunha & Lima, 2008; Yu et al., 2018; Capozziello et al., 2014).

On the other hand, the model-dependent approach, though relatively simpler, gives a much deeper intuition about the evolution of the universe and its constituents. Current observations strongly favour a universe dominated by a cosmic fluid (dark energy) with negative pressure and constant energy density. This is the standard Λ CDM model of cosmology which can propel the accelerated expansion of the universe (Carroll, 2001). Unfortunately, there are still some inconsistencies that the model fails to address. Specifically, the fine-tuning and the coincidence problem (Basilakos & Lima, 2010; Frieman et al., 2008). Therefore, alternate dark energy models such as the XCDM, phantom, quintessence, GCG (generalized chaplygin gas), MCG (modified chaplygin gas) etc. were considered. For example: Melchiorri et al. (2007) used MCMC methods to constrain the parameters in the Λ CDM and other modified Dark energy models. The models iterated through different theoretical assumptions and parameterizations and found a $z_t \in [0.32, 0.48]$ (Melchiorri et al., 2007). Farooq et al. (2016) used Likelihood maximization technique on three different spatially flat and non-flat models (Λ CDM, XCDM, ϕ CDM) with Hubble data from BAO and Cosmic Chronometers. Using different priors on H_0 they found the value of $z_t \in [0.68, 0.88]$ (Farooq et al., 2017). For more methods and models one can refer (Velasquez-Toribio & Magnago, 2020; Wang & Dai, 2006; Farooq & Ratra, 2013).

Following a similar line of thought, we use a model-dependent approach in constraining the transition redshift. In this paper, we use the updated compilation of 32 $H(z)$ data points obtained from cosmic chronometers and the Pantheon+ supernova dataset containing 1701 data points for

eters in the spatially flat and non-flat Λ CDM and XCDM models. *This work improves upon earlier works by including the full covariance matrix for both datasets, which incorporates all statistical and systematic uncertainties*. We use the latest datasets and work with models that directly constrain the transition redshift instead of considering it a derived parameter. Additionally, we plot contours to study the correlations between different model parameters. The paper is organized as follows: In section 2, we describe the Λ CDM and XCDM models. The datasets used and the associated methodology is described in section 3. The final section discusses the results and conclusions of this work.

2 MODELS

In this paper, we have considered four different dark energy models. Using the fact that the second derivative of the scale factor $\ddot{a} = 0$ at the transition epoch, we can derive a relation between the transition redshift and the relative densities of different components in the universe. Using this relation, we can find an equation for the Hubble Parameter in terms of z_t .

2.1 Λ CDM Model

The acceleration equation in the Λ CDM universe dominated by a constant density dark energy is given by:

$$\frac{\ddot{a}}{a} = -\frac{4\pi G}{3} \cdot (\rho_T + 3p_T) \quad (1)$$

ρ_T is the total energy density given by $\rho_T = \frac{\rho_{m0}}{a^3} + \rho_\Lambda$ and p_T is the total pressure density.

Using the equation of state parameter $\omega = 0$ for the matter and $\omega = -1$ for dark energy in the acceleration equation:

$$\frac{\ddot{a}}{a} = -\frac{4\pi G}{3} [\rho_{m0}(1+z)^3 - 2\rho_\Lambda] \quad (2)$$

Using the definition of the transition redshift with $\ddot{a} = 0$ and the equivalence of the energy densities to the normalized energy densities, we obtain z_t as :

$$z_t = \left(\frac{2\Omega_{\Lambda 0}}{\Omega_{m0}} \right)^{\frac{1}{3}} - 1 \quad (3)$$

Here Ω represents the normalized energy densities. For the **Flat Λ CDM model**, the Hubble Parameter is given as:

$$H(z) = H_0 [\Omega_{m0}(1+z)^3 + \Omega_{\Lambda 0}]^{\frac{1}{2}} \quad (4)$$

Substituting for z_t along with $\Omega_{m0} + \Omega_{\Lambda 0} = 1$, we obtain:

$$H(z, f) = H_0 \left[\frac{(1+z)^3}{\frac{1}{2}(1+z_t)^3 + 1} + \frac{(1+z_t)^3}{(1+z_t)^3 + 2} \right]^{\frac{1}{2}} \quad (5)$$

Similarly for the **Non-Flat Λ CDM** model, the Hubble parameter is:

$$H(z, f) = H_0 \left[\Omega_{m0}(1+z)^3 + \Omega_{k0}(1+z)^2 + \Omega_{\Lambda0} \right]^{\frac{1}{2}} \quad (6)$$

Where Ω_{k0} is a space curvature density parameter and z_t for the Non-flat Λ CDM model is now given as:

$$z_t = \left(\frac{2(1 - \Omega_{m0} - \Omega_{k0})}{\Omega_{m0}} \right)^{\frac{1}{3}} - 1 \quad (7)$$

After substituting the value of z_t and using the $\Omega_{m0} + \Omega_{\Lambda0} + \Omega_{k0} = 1$, the Hubble parameter in Non-Flat Λ CDM becomes:

$$H(z, f) = H_0 \left[\frac{(1 - \Omega_{k0})(1+z)^3}{\frac{1}{2}(1+z_t)^3 + 1} + \Omega_{k0}(1+z)^2 + \frac{(1 - \Omega_{k0})(1+z_t)^3}{(1+z_t)^3 + 2} \right]^{\frac{1}{2}} \quad (8)$$

Here, f indicates the **free parameters** H_0 , z_t and Ω_{k0} .

2.2 XCDM Model

In the XCDM model, the dark energy acts as a dynamically evolving fluid. Here, the dark energy fluid pressure p_X and energy density ρ_X are related as:

$$p_X = \omega_X \rho_X \quad (9)$$

where ω_X is the constant equation of state parameter having values less than $-\frac{1}{3}$.

Solutions to the fluid equation result in the energy density given as:

$$\rho_X = \rho_{X0} \left(\frac{a_0}{a} \right)^{3(1+\omega_X)} \quad (10)$$

where the subscript "0" defines the current value of the parameters and thus a_0 is assumed to be unity. Substitution in the acceleration equation gives:

$$\frac{\ddot{a}}{a} = -\frac{4\pi G}{3} \left[\frac{\rho_{m0}}{a^3} + \rho_{X0} \left(\frac{1 + 3\omega_X}{a^{3(1+\omega_X)}} \right) \right] \quad (11)$$

For the flat XCDM model, the condition $\ddot{a} = 0$ results in:

$$z_t = \left[\frac{-\Omega_{m0}}{\Omega_{X0}(1 + 3\omega_X)} \right]^{\frac{1}{3\omega_X}} - 1 \quad (12)$$

Here, Ω_{X0} is the normalized dark energy density.

For the **Flat XCDM model**, the Hubble Parameter equation is:

$$H(z, f) = H_0 \left[\Omega_{m0}(1+z)^3 + \Omega_{X0}(1+z)^{3(1+\omega_X)} \right]^{\frac{1}{2}} \quad (13)$$

Substituting for z_t , along with the condition $\Omega_{m0} + \Omega_{X0} = 1$, we get:

$$H(z, f) = H_0 \left[\frac{(1 + 3\omega_X)(1+z_t)^{3\omega_X}(1+z)^3}{(1 + 3\omega_X)(1+z_t)^{3\omega_X} - 1} + \frac{(1+z)^{3(1+\omega_X)}}{1 - (1 + 3\omega_X)(1+z_t)^{3\omega_X}} \right]^{\frac{1}{2}} \quad (14)$$

For the **Non-Flat Λ CDM model**, the Hubble Parameter can be written as:

$$H(z, f) = H_0 \left[\Omega_{m0}(1+z)^3 + \Omega_{k0}(1+z)^2 + \Omega_{X0}(1+z)^{3(1+\omega_X)} \right]^{\frac{1}{2}} \quad (15)$$

The transition redshift for this model can be written in term of the cosmological parameters as:

$$z_t = \left[\frac{-\Omega_{m0}}{(1 - \Omega_{m0} - \Omega_{k0})(1 + 3\omega_X)} \right]^{\frac{1}{3\omega_X}} - 1 \quad (16)$$

By using the condition $\Omega_{m0} + \Omega_{X0} + \Omega_{k0} = 1$ and substituting the value of z_t in the Hubble parameter equation, we obtain:

$$H(z, f) = H_0 \left[\frac{(1-\Omega_{k0})(1+3\omega_X)(1+z)^3(1+z_t)^{3\omega_X}}{(1+3\omega_X)(1+z_t)^{3\omega_X} - 1} + \Omega_{k0}(1+z)^2 + \frac{(1-\Omega_{k0})(1+z)^{3(1+\omega_X)}}{1-(1+3\omega_X)(1+z_t)^{3\omega_X}} \right]^{\frac{1}{2}} \quad (17)$$

Here, f indicates **free parameters** H_0 , z_t , Ω_{k0} and ω_X .

3 METHODOLOGY AND DATA

In this work, we use the updated 32 Hubble $H(z)$ measurements obtained from passively evolving galaxies in the redshift range $0.07 < z < 1.965$ and the 1701 distance modulus $\mu(z)$ measurements for Supernovae Type Ia in the redshift range $0.001 < z < 2.3$. We determine the best fit values of the parameters in different cosmological models by minimizing the combined χ^2 for the two datasets which is given as:

$$\chi_{total}^2 = \chi_{CC}^2 + \chi_{SNe}^2 \quad (18)$$

We use the publicly available EMCEE (Foreman-Mackey et al., (2013) python package to perform MCMC analysis using flat priors with ranges given in **Table 1**. The analysis gives the joint posterior probability distribution for the model parameters. The distribution is marginalized over other parameters to give an estimate for the maximum likelihood along with the 1σ and 2σ confidence intervals. Finally, we use the CORNER (Foreman-Mackey, 2016) package to plot the 2D confidence contours. The following section describes the observational data sets, statistical methods, and associated errors in detail.

3.1 $H(z)$ data

The Hubble data was obtained from spectroscopic dating of massive, passively evolving low redshift $z \sim 2$ galaxies. Presently, these galaxies contain no active star-formation regions, with most of their stellar mass formed at $z > 1$. Chronometers are important as they measure the Hubble Parameter directly without assuming a particular cosmological model. Fundamentally, this technique determines the differential ages of adjacent pair of galaxies (Δt), given their differential redshift Δz . The ages of these galaxies are directly correlated to the metallicity of their stellar populations. This can be measured by the amplitude of the 4000\AA break in their absorption spectra (Moresco et al., 2016). Finally, the Hubble function is given as:

$$H(z) = \frac{1}{dz} \quad (19)$$

To account for the complete set of systematic uncertainties, we include the full covariance matrix, represented as the sum of statistical and systematic uncertainties. The matrix is given as follows:

$$Cov_{ij} = Cov_{ij}^{stat} + Cov_{ij}^{model} \quad (20)$$

where the systematic effects arise mainly due to the choice of different models used for estimating ages. The model covariance includes errors from the initial mass function (IMF), star formation history (SFH), stellar population synthesis (SPS) model, and stellar metallicity (SM).

$$Cov_{ij}^{model} = Cov_{ij}^{IMF} + Cov_{ij}^{SPS} + Cov_{ij}^{SFH} + Cov_{ij}^{SM} \quad (21)$$

To construct the covariance matrices we use the Mean Percentage Bias ($\widehat{\eta^X}(z)$) table and the following relation from (Moresco et al., 2020).

$$Cov_{ij}^X = \widehat{\eta^X}(z_i) \cdot H(z_i) \cdot \widehat{\eta^X}(z_j) \cdot H(z_j) \quad (22)$$

Where X represents the contribution from different error components. Using the 32 data points, we construct the 32×32 covariance matrix $Cov_{stat+sys}^{-1}$. We now calculate χ^2 and the Likelihood as follows:

$$-2\ln(\mathcal{L}) = \chi_{CC}^2 = \mathbf{\Delta D}^T \cdot Cov_{stat+sys}^{-1} \cdot \mathbf{\Delta D} \quad (23)$$

where $\mathbf{\Delta D}$ is the residual vector defined as: $\mathbf{\Delta D}_i = H^{th}(z_i, \theta) - H^{obs}(z_i)$, $\mathbf{\Delta D}^T$ represents its transpose and θ indicates the model parameters. The H^{th} denotes the Hubble parameter equation for the specific model while H^{obs} is the observed value of the Hubble Parameter.

3.2 Supernova Data

We use the latest Pantheon+ compilation, which analyses 1701 supernova light curves from 1550 distinct supernovae in the redshift range of 0.001 to 2.26. This data includes major contributions from CfA1-4, CSP, DES, PS1, SDSS and SNLS. The observed light curves were fitted using a SALT2 model, which returns the best fit value of the parameters c (color), x_1 (stretch), and x_0 (overall amplitude) (Scolnic et al., 2022). Given the parameters, we can quantify μ_{obs} , the observed distance modulus, using a linear model given as follows:

$$\mu_{obs} = m_B + \alpha x_1 - \beta c - M - \delta_{\mu-bias} \quad (24)$$

The nuisance parameters α , β and M are jointly fitted with the cosmological parameters. Where α and β are the coefficients relating stretch and color to luminosity, M is the absolute magnitude of the supernova and $\delta_{\mu-bias}$ represents the bias correction term. Now

$$m_B \equiv -2.5\log_{10}(x_0) \quad (25)$$

Theoretically the distance modulus is given by:

$$\mu_{th} = 5\log_{10}\left[\frac{D_L}{Mpc}\right] + 25 \quad (26)$$

where D_L , the luminosity distance is defined as:

$$D_L(z) = (1+z) \int_0^z dz' \quad (27)$$

Here c is the speed of light and $H(z)$ is the Hubble parameter equation for different models.

Given μ_{obs} and μ_{th} , the residual is defined as:

$$\Delta \mathbf{D}_i = \mu_{th}(z_i, \theta) - \mu_{obs}(z_i) \quad (28)$$

where θ indicates the model parameters. The log-likelihood or χ^2 relation can now be written as:

$$-2\ln(\mathcal{L}) = \chi_{SNe}^2 = \Delta \mathbf{D}^T \cdot Cov_{stat+sys}^{-1} \cdot \Delta \mathbf{D} \quad (29)$$

$Cov_{stat+sys}^{-1}$ is the 1701×1701 square covariance matrix as described in Brout et al. (2022) (Brout et al., 2022). Because there are 1701 light curves from 1550 SNe, the statistical covariance matrix includes the distance error (σ_μ^2) as the diagonal entry and the measurement noise as the off diagonal terms for duplicate supernovae included in multiple surveys. This compilation improves upon earlier works by accounting for a much larger number of systematic uncertainties. These include errors from the measurement of redshift, peculiar velocities, and host galaxies; calibration of light curves and the SALT2 model fitting; extinction due to the Milky Way; and simulations of survey modeling, distance modulus uncertainty modeling, and intrinsic scatter models.

4 RESULTS

In this paper, we use the updated available $H(z)$ and Supernovae data-sets along with their full covariance matrices to obtain the constraints on the transition redshift, H_0 , and other model parameters such as ω_X and Ω_{k0} . Nuisance parameters α, β and M are also jointly fitted to account for any additional bias. The 2-Dimensional contours and the 1-Dimensional posterior probability distributions for the cosmological parameter are shown in **Figure 1-4**. The best fit values of the model parameters obtained from different datasets are listed in **Table 2**.

- For the Λ CDM model the Hubble parameter H_0 and the transition redshift are tightly constrained. With both the datasets (SNe + CC), the spatially Flat model supports a $H_0 = 73.034_{-0.899}^{0.937}$ and a transition redshift of $z_t = 0.618_{-0.042}^{0.040}$.
While the Non-Flat Λ CDM model supports an open geometry ($\Omega_{k0} = 0.266_{-0.171}^{0.142}$) with a H_0 value of $72.972_{-0.933}^{0.979}$ and a transition redshift of $0.797_{-0.144}^{0.220}$.
- The spatially Flat XCDM model suggest a dynamically evolving fluid ($\omega_X = -0.834_{-0.101}^{0.083}$) with a $H_0 = 72.965_{-0.981}^{0.951}$ and a transition redshift of $0.799_{-0.140}^{0.195}$.
On the other hand, Non-Flat XCDM model also suggests slightly open geometry ($\Omega_{k0} = 0.044_{-0.461}^{0.389}$) with a H_0 value of $72.922_{-1.037}^{1.071}$, a transition redshift of $0.798_{-0.135}^{0.203}$ and an equation of state $\omega_X = -0.863_{-0.313}^{0.167}$.
- The nuisance parameters are consistent across all models with little deviations between the Flat and the Non-Flat models. The parameter α ranges from 0.151 - 0.152, β ranges from 3.014 - 3.030 and M ranges from -19.207 - -19.213.

Parameter	Prior Range
H_0	[50.0, 90.0]
z_t	[0.05, 1.2]
Ω_{k0}	[-0.7, 0.7]
ω_X	[-3.0, 0]
α	[0.05, 0.2]
β	[2, 4]
M	[-19.5, -18.9]

Table 1: Flat priors assumed for the model and nuisance parameters

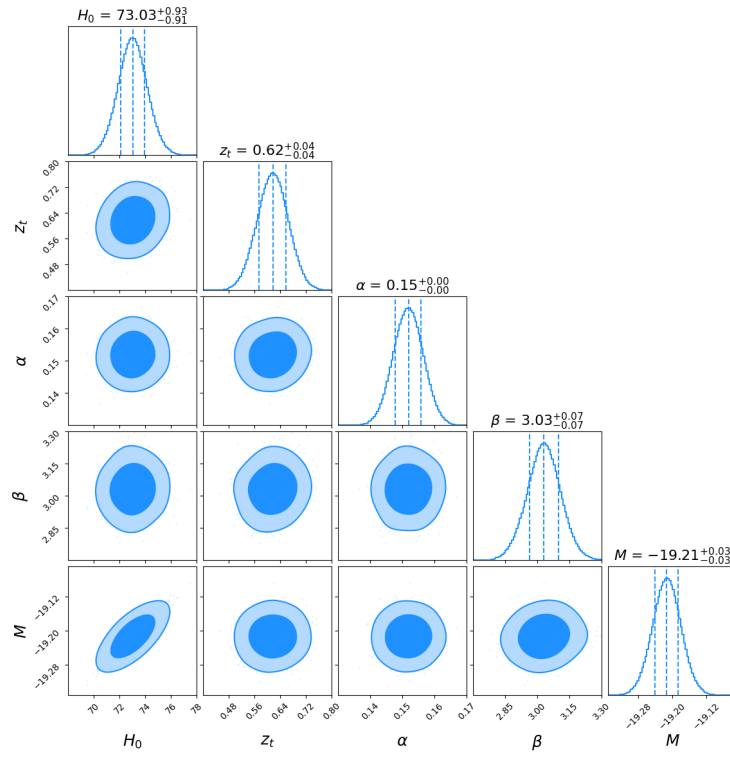


Fig. 1: Joint Confidence Contours for the Flat Λ CDM model with the CC + SNe dataset

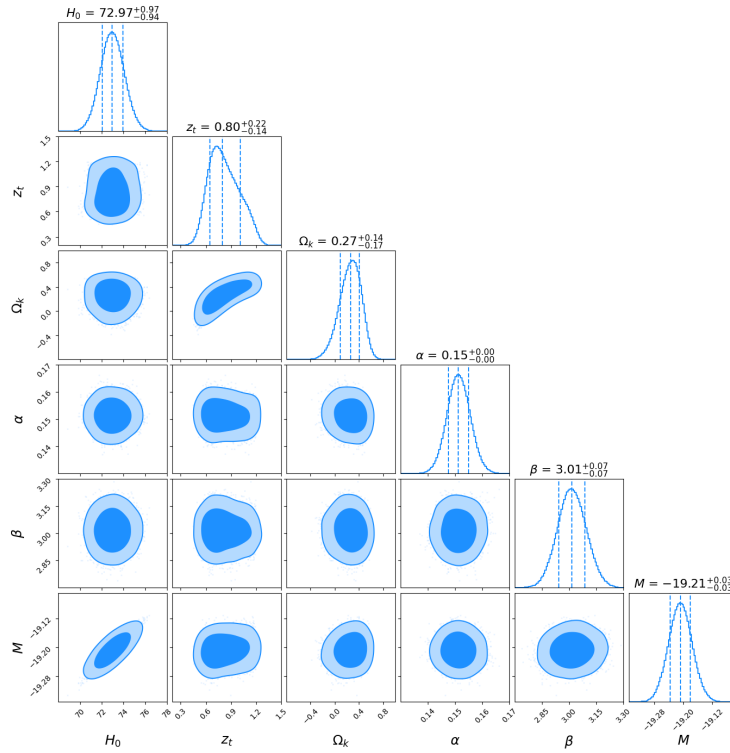


Fig. 2: Joint Confidence Contours for the Non-Flat Λ CDM model with the CC + SNe dataset

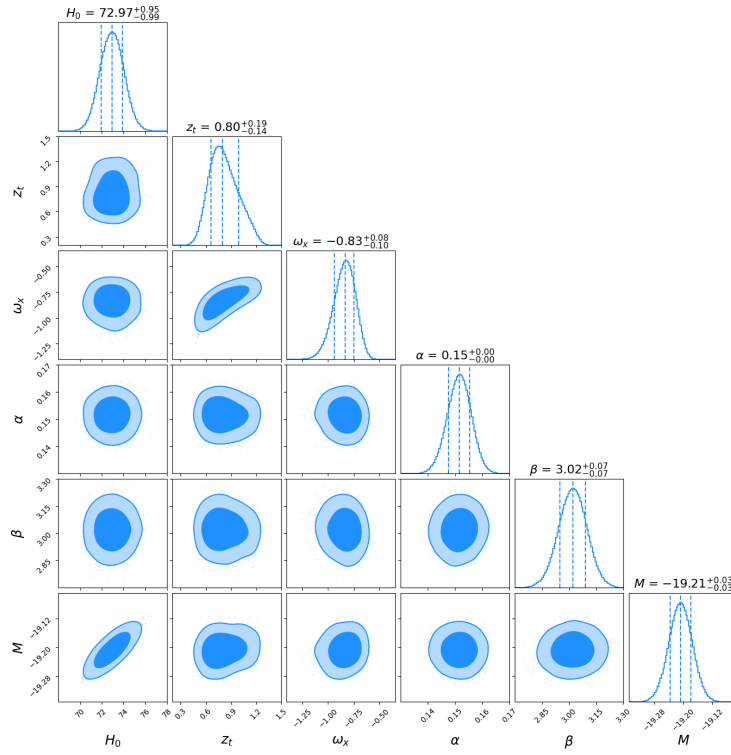


Fig. 3: Joint Confidence Contours for the Flat XCDM model with the CC + SNe dataset

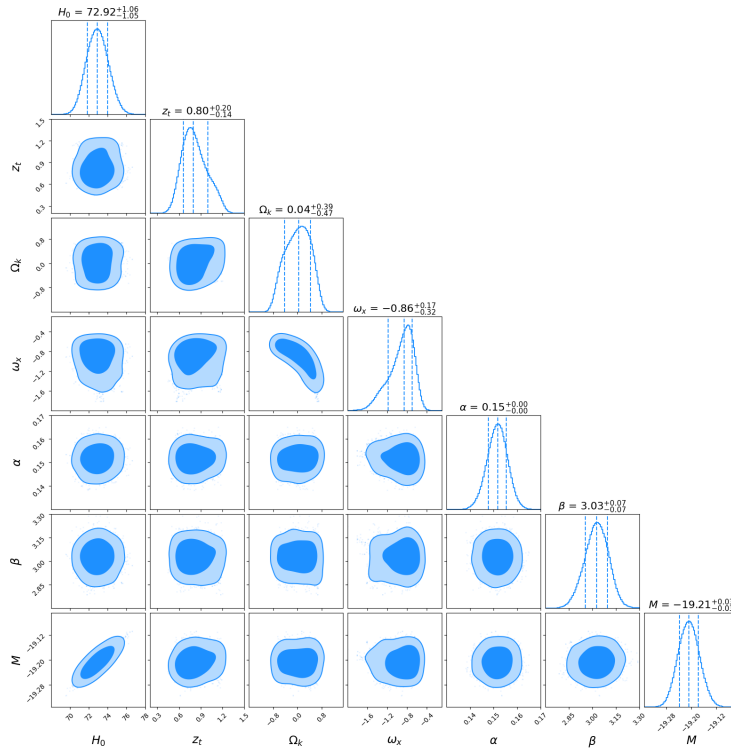


Fig. 4: Joint Confidence Contours for the Non-Flat XCDM model with the CC + SNe dataset

Model	Data Set	H_0	z_t	Ω_{k0}	ω_X	α	β	M
Flat Λ CDM	SNe	$73.500_{-1.013-2.087}^{1.013-2.087}$	$0.587_{-0.043-0.096}^{0.043-0.096}$	-	-	$0.152_{-0.004-0.008}^{0.004-0.008}$	$3.024_{-0.073-0.149}^{0.073-0.149}$	$-19.196_{-0.029-0.060}^{0.029-0.060}$
	CC	$67.841_{-5.392-10.862}^{5.392-10.862}$	$0.621_{-0.163-0.338}^{0.163-0.338}$	-	-	-	-	-
	SNe + CC	$73.034_{-0.937-1.983}^{0.937-1.983}$	$0.618_{-0.040-0.083}^{0.040-0.083}$	-	-	$0.152_{-0.004-0.008}^{0.004-0.008}$	$3.030_{-0.066-0.147}^{0.066-0.147}$	$-19.213_{-0.027-0.057}^{0.027-0.057}$
Non-Flat Λ CDM	SNe	$73.393_{-1.000-2.078}^{1.000-2.078}$	$0.723_{-0.262-0.433}^{0.262-0.433}$	$0.213_{-0.179-0.280}^{0.179-0.280}$	-	$0.151_{-0.004-0.008}^{0.004-0.008}$	$3.019_{-0.073-0.141}^{0.073-0.141}$	$-19.195_{-0.029-0.061}^{0.029-0.061}$
	CC	$66.538_{-5.526-11.782}^{5.526-11.782}$	$0.608_{-0.220-0.490}^{0.220-0.490}$	$0.183_{-0.362-0.494}^{0.362-0.494}$	-	-	-	-
	SNe + CC	$72.972_{-0.979-2.069}^{0.979-2.069}$	$0.797_{-0.033-1.958}^{0.033-1.958}$	$0.266_{-0.149-0.233}^{0.149-0.233}$	-	$0.151_{-0.004-0.008}^{0.004-0.008}$	$3.014_{-0.069-0.145}^{0.069-0.145}$	$-19.208_{-0.028-0.057}^{0.028-0.057}$
Flat χ CDM	SNe	$73.361_{-0.980-2.063}^{0.980-2.063}$	$0.733_{-0.223-0.415}^{0.223-0.415}$	-	$-0.866_{-0.106-0.171}^{0.106-0.171}$	$0.152_{-0.004-0.008}^{0.004-0.008}$	$3.016_{-0.074-0.146}^{0.074-0.146}$	$-19.195_{-0.030-0.062}^{0.030-0.062}$
	CC	$67.321_{-8.644-17.790}^{8.644-17.790}$	$0.566_{-0.241-0.549}^{0.241-0.549}$	-	$-1.005_{-0.516-0.864}^{0.516-0.864}$	-	-	-
	SNe + CC	$72.965_{-0.951-1.972}^{0.951-1.972}$	$0.799_{-0.033-1.957}^{0.033-1.957}$	-	$-0.834_{-0.101-0.218}^{0.083-0.148}$	$0.152_{-0.004-0.008}^{0.004-0.008}$	$3.020_{-0.072-0.151}^{0.071-0.149}$	$-19.208_{-0.028-0.058}^{0.029-0.058}$
Non-Flat χ CDM	SNe	$73.244_{-1.078-2.190}^{1.078-2.190}$	$0.784_{-0.221-0.378}^{0.221-0.378}$	$0.086_{-0.397-0.555}^{0.397-0.555}$	$-0.904_{-0.199-0.288}^{0.199-0.288}$	$0.151_{-0.004-0.008}^{0.004-0.008}$	$3.016_{-0.073-0.152}^{0.071-0.139}$	$-19.199_{-0.031-0.067}^{0.031-0.067}$
	CC	$67.166_{-8.008-18.167}^{8.008-18.167}$	$0.600_{-0.306-0.550}^{0.306-0.550}$	$0.293_{-0.498-0.909}^{0.290-0.392}$	$-1.162_{-0.663-1.023}^{0.663-1.023}$	-	-	-
	SNe + CC	$72.922_{-1.037-1.959}^{1.037-1.959}$	$0.798_{-0.203-0.368}^{0.203-0.368}$	$0.044_{-0.389-0.604}^{0.389-0.604}$	$-0.863_{-0.313-0.625}^{0.167-0.254}$	$0.152_{-0.004-0.007}^{0.004-0.008}$	$3.028_{-0.067-0.135}^{0.067-0.135}$	$-19.207_{-0.031-0.058}^{0.029-0.061}$

Table 2: 1σ and 2σ C.L. constraints on the model parameters

5 DISCUSSION

In this paper, we focus on constraining the transition redshift and build on previous works by using updated datasets with full covariance matrices and additional dark energy models. We express the Hubble parameter equation of dark energy models in term of z_t and using the MCMC technique, obtain the contours between different model parameters. We observe that, compared to the $H(z)$ data, the SNe data predicts an early time transition (except for the Λ CDM model). Since we observe positive correlations between z_t and other cosmological parameter (Ω_{k0}, ω_X) from the confidence contours, we can hypothesize that the exception of Λ CDM model could be a consequence of these correlations. More research is needed to substantiate this claim, nonetheless all models support z_t in the intermediate redshift range [0.61-0.79]. These results agree with past results obtained from other datasets and methodologies (mentioned in **Table 3**). We find negligible difference in the best fit values of SNe Ia parameters in each dark energy model studied in this work. Additionally, the constrained nuisance parameters are also consistent with the results obtained earlier in the literature (Betoule, M. et al., 2014; Chen et al., 2022).

The obtained value of current Hubble Parameter (H_0) differ for the two datasets, further supporting the Hubble tension. The $H(z)$ data supports lower values of H_0 which is in concordance with the Planck CMB results while the Pantheon+ dataset support higher value of H_0 which again support the results earlier obtained with the SNe dataset.(Aghanim et al., 2020; Riess et al., 2016).

For all the Non-Flat models considered in the paper, the non-flat Λ CDM suggests a moderately open geometry ($\Omega_{k0} > 0$) but is still consistent with a spatially flat universe within 2σ limits. Similar observations of the curvature parameter were observed earlier by (Farooq et al., 2017; Yang & Gong, 2021). The Non-Flat XCDM model, on the other hand, indicates a very mild deviation from a Flat Universe but has larger error bounds on the curvature density of the universe.

For the dynamical dark energy models, there is mild variation in the equation of state parameter ($\omega_X \neq -1$). Nonetheless, the Λ CDM model ($\omega_X = -1$) can be easily recovered within 2σ levels. Our results are consistent with those obtained recently with the Pantheon+ compilation (Brout et al., 2022) and the 2019 DES Compilation (Abbott et al., 2019).

As mentioned above, the Non-Flat models support an open geometry, although, the Non-Flat Λ CDM model indicates a much stronger positive curvature ($\Omega_{k0} = 0$ is 2σ away) as compared to the XCDM model ($\Omega_{k0} = 0$ is 1σ away). This shows that, when the equation of state is allowed to vary, a flat universe is more statistically probable. Thus, a strong negative correlation exists between the dark energy equation of state and the curvature density which can also be seen in confidence contours for the Non-flat XCDM model (**Figure 4**). This degeneracy is further discussed in (Clarkson et al., 2007; Ichikawa et al., 2006) which explore models with different assumptions and discuss the importance of constraining dark energy models in association with the curvature. They also mention the implications of assuming zero curvature on the equation of state parameter. More information on this degeneracy can be found in (Huang et al., 2007; Polarski & Ranquet,

Finally, we observe that using the combined, updated datasets of $H(z)$ and SNe along with their full covariance matrices, the best fit value of transition redshift lies in the range $0.618 < z_t < 0.799$ for all four dark energy models with the standard Flat Λ CDM model having the lowest error bars compared to other models. These results are in general agreement with past analyses and the Planck's results within 2σ level.

Method	Models	Data Set	z_t	References	
Likelihood Maximization	KM: $q(z)$	SNe(SNLS)	0.61	(Cunha & Lima, 2008)	
	KM: $\omega(z)$	BAO + CMB(WMAP) + SNe(Union)	0.7 - 1	(Magaña et al., 2014)	
	KM: $q(z)$	Age of Galaxies + Strong Lensing + SNe(JLA)	0.6 - 0.98	(Rani et al., (2015)	
	KM: $H(z)$, $D_C(z)$, $q(z)$	CC + SNe(JLA)	0.806 - 0.973	(J.F. Jesus et al., 2018)	
	KM: $q(z)$	CC + BAO + SNe(Pantheon) + CMB	0.593 - 0.792	(Al Mamon, 2021)	
	Λ CDM Model		CC	0.64	(Moresco et al., 2016)
			CC + BAO	0.723 - 0.832	(Farooq et al., 2017; Farooq & Ratra, 2013)
			CC + BAO + SNe(Pantheon)	0.69	(Velasquez-Toribio & Magnago, 2020)
			CC + SNe (Pantheon+)	0.61 - 0.82	Present Work
	CF: $H(z)$	CC + BAO + SNe(Pantheon)	0.6857	(Koussour et al., 2022)	
	CF: $H(z)$, $q(z)$, $j(z)$	CC + BAO + SNe(Union)	0.77 - 0.86	(Capozziello et al., 2014)	
	CF: $a(t)$	BAO + SNe(Union2.1)	0.28 - 0.63	(Muthukrishna & Parkinson, 2016)	
	CF: $H(z)$, $q(z)$	SNe (Pantheon) + BAO + GRB	0.739 - 0.831	(Muccino et al., 2022)	
	XCDM Model		CC + BAO	0.684 - 0.813	(Farooq et al., 2017; Farooq & Ratra, 2013)
		CC + SNe(Pantheon+)	0.77 - 0.79	Present Work	
ϕ CDM Model		CC + BAO	0.690 - 0.885	(Farooq et al., 2017; Farooq & Ratra, 2013)	
Regression	GP: $H(z)$, $D_L(z)$	CC + SNe(Pantheon)	0.57 - 0.69	(Jesus et al., 2020)	
	GP: $H(z)$, $q(z)$	CC + BAO	0.637 - 0.71	(Velasquez-Toribio & Fabris, 2021)	
	GP: $q(z)$	CC + SNe(Pantheon)	0.61	(Yang & Gong, 2020)	
	GP: $H(z)$	CC + BAO	0.44 - 0.65	(Yu et al., 2018)	
	WFR: $q(z)$, $j(z)$	CC + BAO + SNe(Pantheon + MCT)	0.8	(Gómez-Valent, 2019)	
	LOESS+SIMEX	Age of Galaxies + Strong Lensing + SNe(JLA)	0.7	(Rani et al., (2015)	

Table 3: A summary of the current constraint on the transition redshift obtained from different works. (KM: Kinematic Models, CF: Cosmographic Functions, GP: Gaussian Process, WFR: Weighted Function Regression)

ACKNOWLEDGEMENTS

One of the author (David Dahiya) thanks the Principal, Deen Dayal Upadhyaya College, for providing the facilities where part of the work was done.

References

- Abbott, T. M. C., Alarcon, A., Allam, S., et al. 2019, Phys. Rev. Lett., 122, 171301 12
- Aghanim et al., N. 2020, Astronomy & Astrophysics, 641, A6 12
- Al Mamon, A. 2021, Modern Physics Letters A, 36, 2150049 2, 14
- Basilakos, S., & Lima, J. A. S. 2010, Phys. Rev. D, 82, 023504 2
- Betoule, M., Kessler, R., Guy, J., et al. 2014, A&A, 568, A22 12

- Capozziello, S., Dunsby, P. K. S., & Luongo, O. 2021, *Monthly Notices of the Royal Astronomical Society*, 509, 5399 2
- Capozziello, S., Farooq, O., Luongo, O., & Ratra, B. 2014, *Phys. Rev. D*, 90, 044016 2, 14
- Carroll, S. M. 2001, *Living reviews in relativity*, 4, 1 2
- Chen, R., Scolnic, D., Rozo, E., et al. 2022, *The Astrophysical Journal*, 938, 62 12
- Clarkson, C., Cortês, M., & Bassett, B. 2007, *Journal of Cosmology and Astroparticle Physics*, 2007, 011 12
- Cunha, J. V., & Lima, J. A. S. 2008, *Monthly Notices of the Royal Astronomical Society*, 390, 210 2, 14
- Farooq, O., Madiyar, F. R., Crandall, S., & Ratra, B. 2017, *The Astrophysical Journal*, 835, 26 2, 12, 14
- Farooq, O., & Ratra, B. 2013, *The Astrophysical Journal Letters*, 766, L7 2, 14
- Foreman-Mackey, D. 2016, *The Journal of Open Source Software*, 1, 24 5
- Foreman-Mackey, D., Hogg, D. W., Lang, D., & Goodman, J. (2013), *Publications of the Astronomical Society of the Pacific*, 125, 306 5
- Frieman, J. A., Turner, M. S., & Huterer, D. 2008, *Annual Review of Astronomy and Astrophysics*, 46, 385 2
- Gómez-Valent, A. 2019, *Journal of Cosmology and Astroparticle Physics*, 2019, 026 14
- Huang, Z.-Y., Wang, B., & Su, R.-K. 2007, *International Journal of Modern Physics A*, 22, 1819 12
- Ichikawa, K., Kawasaki, M., Sekiguchi, T., & Takahashi, T. 2006, *Journal of Cosmology and Astroparticle Physics*, 2006, 005 12
- Jesus, J., Valentim, R., Escobal, A., & Pereira, S. 2020, *Journal of Cosmology and Astroparticle Physics*, 2004, 053 2, 14
- J.F. Jesus, R.F.L. Holanda, & S.H. Pereira. 2018, *Journal of Cosmology and Astroparticle Physics*, 1805, 073 2, 14
- Koussour, M., Pacif, S. K. J., Bennai, M., & Sahoo, P. K. 2022, arXiv:2208.04723 2, 14
- Kumar, D., Jain, D., Mahajan, S., Mukherjee, A., & Rana, A. 2022, arXiv:2205.13247 2
- Lima, J. A. S., Jesus, J. F., Santos, R. C., & Gill, M. S. S. 2012, Is the transition redshift a new cosmological number?, arXiv:1205.4688 1
- Magaña, J., Cárdenas, V. H., & Motta, V. 2014, *Journal of Cosmology and Astroparticle Physics*, 1410, 017 14
- Melchiorri, A., Pagano, L., & Pandolfi, S. 2007, *Phys. Rev. D*, 76, 041301 1, 2
- Moresco, M., Jimenez, R., Verde, L., Cimatti, A., & Pozzetti, L. 2020, *The Astrophysical Journal*, 898, 82 6
- Moresco, M., Pozzetti, L., Cimatti, A., et al. 2016, *Journal of Cosmology and Astroparticle Physics*, 1605, 014 5, 14
- Muccino, M., Luongo, O., & Jain, D. 2022, Constraints on the transition redshift from the calibrated Gamma-ray Burst E_p - E_{iso} correlation, arXiv:2205.13247 2, 14

- Muthukrishna, D., & Parkinson, D. 2016, *Journal of Cosmology and Astroparticle Physics*, 2016, 052 14
- Perlmutter et al., S. 1999, *The Astrophysical Journal*, 517, 565 1
- Polarski, D., & Ranquet, A. 2005, *Physics Letters B*, 627, 1 12
- Rani, N., Jain, D., Mahajan, S., Mukherjee, A., & Pires, N. (2015), *Journal of Cosmology and Astroparticle Physics*, 1512, 045 2, 14
- Riess, A. G., Macri, L. M., Hoffmann, S. L., et al. 2016, *The Astrophysical Journal*, 826, 56 12
- Riess et al., A. G. 1998, *The Astronomical Journal*, 116, 1009 1
- Scolnic, D., Brout, D., Carr, A., et al. 2022, *The Astrophysical Journal*, 938, 113 6
- Seikel, M., Clarkson, C., & Smith, M. 2012, *Journal of Cosmology and Astroparticle Physics*, 2012, 036 2
- Velasquez-Toribio, A. M., & Fabris, J. C. 2021, *Constraints on Cosmographic Functions of Cosmic Chronometers Data Using Gaussian Processes*, arXiv:2104.07356 2, 14
- Velasquez-Toribio, M. A., & Magnago, A. d. R. 2020, *Observational constraints on the non-flat Λ CDM model and a null test using the transition redshift*, arXiv:2001.04645 2, 14
- Wang, F.-Y., & Dai, Z.-G. 2006, *Chinese Journal of Astronomy and Astrophysics*, 6, 561 2
- Yang, Y., & Gong, Y. 2020, *Journal of Cosmology and Astroparticle Physics*, 2020, 059 14
- Yang, Y., & Gong, Y. 2021, *Monthly Notices of the Royal Astronomical Society*, 504, 3092 12
- Yu, H., Ratra, B., & Wang, F.-Y. 2018, *The Astrophysical Journal*, 856, 3 2, 14
- Çamlıbel, A. K., İbrahim Semiz, & Feyizoğlu, M. A. 2020, *Classical and Quantum Gravity*, 37, 235001 2